Journal of Statistical Mechanics: Theory and Experiment
An IOP and SISSA journal

Computer simulations of an impurity in a granular gas under planar Couette flow

F Vega Reyes, A Santos and V Garzó

Departamento de Física, Universidad de Extremadura, E-06071 Badajoz, Spain
E-mail: fvega@unex.es, andres@unex.es and vicenteg@unex.es

Received 10 May 2011
Accepted 16 June 2011
Published 12 July 2011

Online at stacks.iop.org/JSTAT/2011/P07005
doi:10.1088/1742-5468/2011/07/P07005

Abstract. We present in this work results from numerical solutions, obtained by means of the direct simulation Monte Carlo (DSMC) method, of the Boltzmann and Boltzmann–Lorentz equations for an impurity immersed in a granular gas under planar Couette flow. The DSMC results are compared with the exact solution of a recent kinetic model for the same problem. The results confirm that, in steady states and over a wide range of parameter values, the state of the impurity is enslaved to that of the host gas: it follows the same flow velocity profile, its concentration (relative to that of the granular gas) is constant in the bulk region, and the impurity/gas temperature ratio is also constant. We determine also the rheological properties and nonlinear hydrodynamic transport coefficients for the impurity, finding a good semi-quantitative agreement between the DSMC results and the theoretical predictions.

Keywords: granular matter, kinetic theory of gases and liquids, rheology and transport properties, Boltzmann equation

ArXiv ePrint: 1105.1742

1742-5468/11/P07005+24$33.00

Contents

1. Introduction

The transport of granular matter has a growing interest for industrial and technological purposes. For this reason, it is convenient to study the behavior of simplified granular systems, from both an experimental and a theoretical point of view (see [1], for example, for a recent review on the field). Some of the phenomena of interest for industrial applications are the behavior of transport, diffusion, and segregation of grains depending on their different physical properties (mass, form, size, or inelasticity) [2]–[16]. When the granular medium is dilute and vigorously shaken, the motion of grains resembles that of atoms or molecules in an ordinary gas and the near-instantaneous binary collisions prevail. Under these conditions, kinetic theory properly modified to account for the inelasticity of collisions provides a useful framework for analyzing granular flows. It has been shown that the corresponding kinetic equation describing the statistics of this many-particle system can generate the so-called 'normal solution', in which all the spatial dependence occurs through the average fields [17]. In this situation, the fluxes can also be expressed as functions of the average fields and this results in a closed set of equations for the average fields that define a hydrodynamic description since it is formally equivalent to the hydrodynamic description in classical fluid mechanics [18]. Moreover, if the spatial gradients are supposed to be small enough, the hydrodynamics is Newtonian and the resulting equations are the Navier–Stokes (NS) ones [17, 19]. Therefore, there have been attempts to determine the NS transport coefficients of granular mixtures in the low density regime [8, 20, 21] and also at moderate densities [22]–[29].

J. Stat. Mech. (2011) P07005

On the other hand, the inelasticity in the collisions (i.e., the kinetic energy loss in interparticle collisions) introduces an inherent time scale that results, if a steady state needs to be maintained, in a minimum size of the gradients as a function of the degree of inelasticity [30]. This renders the NS approach not appropriate for most steady rapid granular flows. In fact, we already know that, for example, the simple shear flow for a granular gas [31]–[33] is inherently non-Newtonian [34]. In addition, previous works on the latter flow have shown that nonlinear effects can significantly modify segregation criteria with respect to NS hydrodynamic theories [15].

Obviously, the determination of non-Newtonian hydrodynamic profiles and transport coefficients is a prerequisite for a more complete description of transport and segregation of impurities immersed in a granular gas. This fact motivated a previous work by the authors, in which, via a kinetic model for a multicomponent granular gas [35], we determined an exact analytical solution of the problem of the steady planar Couette flow for an impurity in a low density granular gas [36]. This solution presents the advantage of including terms of all orders in the velocity and temperature spatial gradients, thus capturing nonlinear effects such as normal stress differences and a heat flux component normal to the thermal gradient. On the other hand, recent theory results on monocomponent granular gases have revealed new and interesting classes of flows that support the validity of a hydrodynamic description, without the restriction of small spatial gradients [37]–[42]. It is thus interesting (a) to check whether the hydrodynamic profiles found in the kinetic model description are shared by the true Boltzmann equation and (b) to gauge the degree of accuracy of the analytical solution derived in [36].

This has motivated the present work, where by means of the direct simulation Monte Carlo (DSMC) method [43] we obtain the numerical solution of the Boltzmann equation associated with a smooth hard-sphere impurity immersed in a low density gas of inelastic smooth hard spheres under Couette flow. As in the case of the kinetic model, the DSMC solution is in principle not restricted to small spatial gradients [43].

Let us consider a set of identical smooth hard spheres (of diameter σ_2 and mass m_2) that collide inelastically with each other. The inelasticity of collisions is characterized by a constant coefficient of normal restitution α_2. We will consider that the number density of the system is sufficiently low that the typical contact times at collisions are much smaller than the typical time interval between collisions. In this low density regime, one can neglect the velocity correlations between the particles that are about to collide (the 'molecular chaos' hypothesis). In these conditions, as for an ordinary gas of hard spheres, we can describe statistically this granular gas through the Boltzmann equation conveniently adapted to take into account the inelasticity in the collisions [19, 44, 45]. The granular gas is enclosed between two infinite parallel walls, here assumed to be both at the same temperature T_{w}, moving with a relative velocity U. In this way, the sheared granular gas reaches a steady state with a non-zero velocity profile. The base laminar flows in this geometry (see figure 1) should be of the form $\mathbf{u}_2 = u_{2,x}(y)\mathbf{e}_x$. Moreover, a temperature profile $T_2(y)$ and a density profile $n_2(y)$ are present. We introduce now another set of inelastic smooth hard spheres (of diameter σ_1 and mass m_1). The concentration of this new species is assumed to be negligible, i.e., its density (n_1) relative to that of the granular gas (n_2) tends to zero: $x_1 = n_1/n_2 \to 0$ (tracer limit). For this reason we call the 'impurity' granular species number 1. The inelasticity of a collision between a sphere of species 1 and a sphere of species 2 is characterized by a constant coefficient of normal restitution α_1,

J. Stat. Mech. (2011) P07005

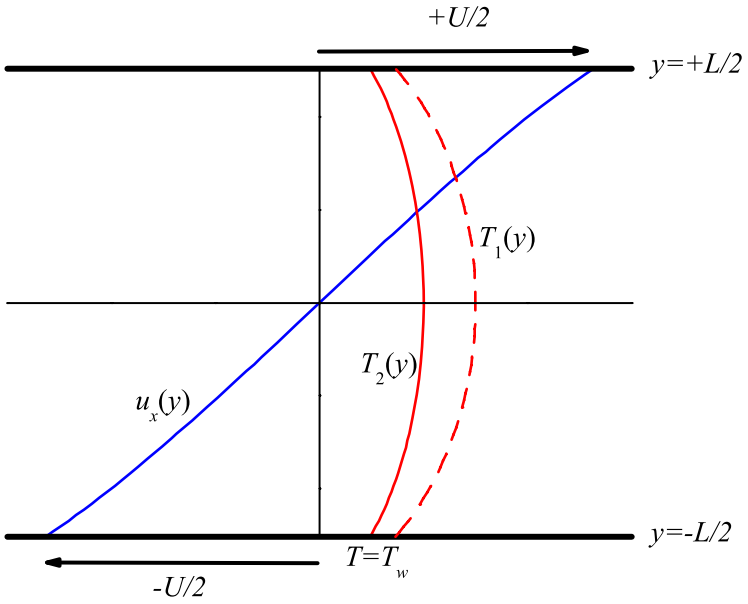

Figure 1. Sketch of the planar Couette flow. The granular gas and the impurity are enclosed between two infinite parallel walls located at $y = \pm L/2$, moving along the x-direction with velocities $\pm U/2$, and kept at the temperature $T_{\rm w}$. In the steady state, the granular gas and the impurity move with the same flow velocity and show different temperature profiles, $T_2(y)$ and $T_1(y)$, respectively, but with constant ratio $\chi \equiv T_1/T_2$.

which in general differs from α_2. Due to the shearing from the boundaries, the impurity species will also reach a base steady flow of the same type as that of the granular gas, i.e., $\mathbf{u}_1 = u_{1,x}(y)\mathbf{e}_x$, $T_1(y)$, and $n_1(y)$.

From the exact solution to the kinetic model mentioned above, one finds that the hydrodynamic profiles satisfy the following properties. Regarding the excess component (host granular gas) [46], (i) the pressure $p_2 = n_2 T_2$ is uniform, (ii) the (local) shear rate $\partial u_{2,x}/\partial y$ scaled with respect to the (local) collision frequency $\nu_2 \propto n_2 T_2^{1/2}$ is uniform, and (iii) the temperature T_2 is a parabolic function of the flow velocity $u_{2,x}$. In the case of the tracer component (impurity), one finds that [36] (iv) the flow velocity coincides with that of the gas, i.e., $u_{1,x} = u_{2,x}$, (v) the mole fraction n_1/n_2 is uniform, and (vi) the temperature ratio $\chi \equiv T_1/T_2$ is also uniform. As we said above, the main goal of the paper is to confirm these predictions by means of computer simulations. In addition, we will measure the momentum and heat fluxes of the impurity to get the generalized transport coefficients and compare them with the analytical results derived from the kinetic model.

The structure of the paper is the following. We formally describe the kinetic theory problem in section 2, where the generalized rheological and transport coefficients are also defined. In this section 2 we also briefly recall the kinetic model results and describe the numerical method (DSMC). In section 3 we present the simulation data compared with the analytical solution of the kinetic model and discuss the results. Finally, we present the conclusions in section 4. Additionally, we present in the appendix the theoretical hydrodynamic properties for the impurity from our previous work [36].

J. Stat. Mech. (2011) P07005

2. The theoretical description and numerical methods

2.1. The Boltzmann description of the Couette flow for the granular gas and the impurity

We consider a granular gas composed of inelastic d-dimensional hard spheres of diameter σ_2, mass m_2, and coefficient of normal restitution α_2. In the low density regime, the corresponding velocity distribution function $f_2(\mathbf{r},\mathbf{v},t)$ (in the absence of gravity) obeys the Boltzmann equation

$$(\partial_t + \mathbf{v}\cdot\nabla)\, f_2 = J_{22}[\mathbf{v}|f_2,f_2], \tag{2.1}$$

where $J_{22}[\mathbf{v}|f_2,f_2]$ is the (inelastic) collision operator.

We add now the impurity particles of diameter σ_1 and mass m_1 (species 1), which are present in a vanishing concentration. For this reason, we can assume that collisions between impurity particles themselves may be neglected and, in addition, the state of the granular gas (species 2) is not affected by the presence of impurities, so equation (2.1) is still valid. The velocity distribution function $f_1(\mathbf{r},\mathbf{v},t)$ for the impurity particles obeys the Boltzmann–Lorentz equation

$$(\partial_t + \mathbf{v}\cdot\nabla)\, f_1 = J_{12}[\mathbf{v}|f_1,f_2], \tag{2.2}$$

where $J_{12}[\mathbf{v}|f_1,f_2]$ is the corresponding (inelastic) collision operator, which is parameterized by the impurity–gas coefficient of normal restitution α_1. Detailed expressions for $J_{ij}[\mathbf{v}|f_i,f_j]$ can be found in, for instance, [35].

The relevant hydrodynamic fields for both species are the number densities n_i, flow velocities $\mathbf{u}_i$, and granular temperatures T_i. They are defined by the relations

$$n_i(\mathbf{r},t) = \int d\mathbf{v}\, f_i(\mathbf{r},\mathbf{v},t), \tag{2.3}$$

$$\mathbf{u}_i(\mathbf{r},t) = \frac{1}{n_i(\mathbf{r},t)}\int d\mathbf{v}\,\mathbf{v} f_i(\mathbf{r},\mathbf{v},t), \tag{2.4}$$

$$T_i(\mathbf{r},t) = \frac{m_i}{dn_i(\mathbf{r},t)}\int d\mathbf{v}\,[\mathbf{v}-\mathbf{u}_i(\mathbf{r},t)]^2 f_i(\mathbf{r},\mathbf{v},t). \tag{2.5}$$

In equation (2.5) we have defined the partial temperatures T_i taking the velocities of species i relative to the mean value $\mathbf{u}_i$. The usual choice, however, is to refer the velocities to the global mean flow velocity $\mathbf{u}$ [36]. Here, for convenience, we adopt the former choice. In any case, since $\mathbf{u}=\mathbf{u}_2$ in the tracer limit, the two choices are equivalent in the case of the granular gas. Additionally, the pressure tensor P_i and the heat flux $\mathbf{q}_i$ for each species can be defined as

$$\mathsf{P}_i(\mathbf{r},t) = m_i\int d\mathbf{v}\,[\mathbf{v}-\mathbf{u}_i(\mathbf{r},t)]\,[\mathbf{v}-\mathbf{u}_i(\mathbf{r},t)]\, f_i(\mathbf{r},\mathbf{v},t), \tag{2.6}$$

$$\mathbf{q}_i(\mathbf{r},t) = \frac{m_i}{2}\int d\mathbf{v}\,[\mathbf{v}-\mathbf{u}_i(\mathbf{r},t)]^2\,[\mathbf{v}-\mathbf{u}_i(\mathbf{r},t)]\, f_i(\mathbf{r},\mathbf{v},t). \tag{2.7}$$

Given that the microscopic state of the granular gas is independent of the microscopic state of the impurities, the mass, momentum, and energy balance equations for species

J. Stat. Mech. (2011) P07005

2 take the usual form [17]

$$D_t n_2 + n_2 \nabla \cdot \mathbf{u}_2 = 0, \tag{2.8}$$

$$D_t \mathbf{u}_2 + \frac{1}{m_2 n_2} \nabla \cdot \mathsf{P}_2 = \mathbf{0}, \tag{2.9}$$

$$D_t T_2 + \frac{2}{d n_2} \left(\nabla \cdot \mathbf{q}_2 + \mathsf{P}_2 : \nabla \mathbf{u}_2 \right) = -\zeta_2 T_2, \tag{2.10}$$

where $D_t \equiv \partial_t + \mathbf{u}_2 \cdot \nabla$ is the material time derivative and

$$\zeta_2 = -\frac{m_2}{d n_2} \int d\mathbf{v}\, v^2 J_{22}[\mathbf{v}|f_2, f_2] \tag{2.11}$$

is the cooling rate of the granular gas.

Now we assume that the system (granular gas plus impurities) is subject to the planar Couette flow. For steady states ($\partial_t = 0$), and given the geometry of the problem ($\partial_x = \partial_z = 0$), we obtain

$$\partial_y P_{2,xy} = \partial_y P_{2,yy} = 0, \tag{2.12}$$

$$\partial_y q_{2,y} + P_{2,xy} \partial_y u_{2,x} = -\frac{d}{2} \zeta_2 n_2 T_2. \tag{2.13}$$

Thus far, all the equations in this section are formally exact in the framework of the Boltzmann equation. On the basis of previous results [36, 46] derived from the kinetic model described below, we expect the hydrodynamic fields of the gas in the bulk domain of the system to have the forms

$$p_2 = n_2 T_2 = \text{const}, \tag{2.14}$$

$$\frac{1}{\nu_2} \partial_y u_{2,x} = a = \text{const}, \tag{2.15}$$

$$\frac{1}{2 m_2 Pr} \left(\frac{1}{\nu_2} \partial_y \right)^2 T_2 = -\gamma = \text{const}. \tag{2.16}$$

Here, $Pr = (d-1)/d$ is the conventional Prandtl number [18] and $\nu_2 \propto n_2 T_2^{1/2}$ is a characteristic collision frequency. For the sake of concreteness, henceforth we will take

$$\nu_2 \equiv \frac{8\pi^{(d-1)/2}}{(d+2)\Gamma(d/2)} n_2 \sigma_2^{d-1} \left(T_2/m_2 \right)^{1/2}. \tag{2.17}$$

In equation (2.15), the constant a represents a dimensionless shear rate. It plays the role of a Knudsen number associated with the velocity gradient. The constant γ in equation (2.16) is a dimensionless parameter (henceforth called thermal curvature coefficient) characterizing the curvature of the temperature profile as a consequence of both the viscous heating and the collisional cooling. As a consequence, γ must depend on both the shear rate a and the coefficient of restitution α_2. It is interesting to note that, from equations (2.15) and (2.16), one finds

$$T_2(y) = T_2(0) - Pr \frac{m_2 \gamma}{a^2} u_{2,x}^2(y), \tag{2.18}$$

J. Stat. Mech. (2011) P07005

where we have considered that $u_{2,x}(0) = 0$ and the temperature profile is symmetric. Equation (2.18) implies that, if eliminating y between T_2 and $u_{2,x}$, the temperature is a linear function of $u_{2,x}^2$.

With respect to the state of the impurities, we assume that it is enslaved to that of the gas. This means that [36]

$$\mathbf{u}_1 = \mathbf{u}_2, \tag{2.19}$$

$$x_1 \equiv \frac{n_1}{n_2} = \text{const}, \tag{2.20}$$

$$\chi \equiv \frac{T_1}{T_2} = \text{const}. \tag{2.21}$$

The hypothesis (2.19) implies that there is no diffusion of the impurities with respect to the gas particles. Equations (2.20) and (2.21), together with equation (2.14), imply that $p_1 = n_1 T_1 = \text{const}$. In summary, the hydrodynamic profiles of the system are provided by equations (2.14)–(2.16) and (2.19)–(2.21).

In order to characterize the non-Newtonian properties, it is convenient to introduce the following five dimensionless rheological factors [36, 41, 42, 46]:

$$P_{i,xy} = -\eta_i^*(a)\frac{n_i T_i}{\nu_i}\frac{\partial u_{i,x}}{\partial y}, \tag{2.22}$$

$$\theta_{i,x}(a) = \frac{P_{i,xx}}{n_i T_i}, \qquad \theta_{i,y}(a) = \frac{P_{i,yy}}{n_i T_i}, \tag{2.23}$$

$$q_{i,y} = -\lambda_i^*(a)\frac{d+2}{2m_i Pr}\frac{n_i T_i}{\nu_i}\frac{\partial T_i}{\partial y}, \tag{2.24}$$

$$q_{i,x} = \phi_i^*(a)\frac{d+2}{2m_i Pr}\frac{n_i T_i}{\nu_i}\frac{\partial T_i}{\partial y}, \tag{2.25}$$

where ν_2 is defined by equation (2.17) and

$$\nu_1 \equiv \frac{4\pi^{(d-1)/2}}{(d+2)\Gamma(d/2)} n_2 \sigma_{12}^{d-1}\left(\frac{2T_1}{m_1} + \frac{2T_2}{m_2}\right)^{1/2}. \tag{2.26}$$

Note that, in the case $i = 1$, the definitions of η_i^*, λ_i^*, and ϕ_i^* in equations (2.22), (2.24), and (2.25) slightly differ from those in [36]. The nondimensionalization of the generalized shear viscosity η_i^* and thermal conductivity λ_i^* is such that $\eta_2^* = \lambda_2^* = 1$ for an elastic gas ($\alpha_2 = 1$) in the NS regime ($a \to 0$) [18]. Note that, while η_i^* and λ_i^* are generalizations of NS transport coefficients, the functions $\theta_{i,x}$, $\theta_{i,y}$, and ϕ_i^* are generalizations of Burnett transport coefficients [18, 47, 48].

Of course, if the impurities are mechanically equivalent to the gas particles (i.e., $m_1 = m_2$, $\sigma_1 = \sigma_2$, and $\alpha_1 = \alpha_2$), the transport coefficients associated with the two species coincide.

Taking into account the constitutive forms (2.22) and (2.24) for the granular gas ($i = 2$), as well as equations (2.14)–(2.16), the exact balance equation (2.13) becomes

$$\eta_2^* a^2 - (d+2)\lambda_2^*\gamma = \frac{d}{2}\zeta_2^*, \qquad \zeta_2^* \equiv \frac{\zeta_2}{\nu_2}. \tag{2.27}$$

J. Stat. Mech. (2011) P07005

Note that in the elastic case ($\zeta_2^* = 0$) and in the NS limit (i.e., $\eta_2^* \to 1$ and $\lambda_2^* \to 1$) one has $\gamma = a^2/(d+2)$ [49]. In general, γ depends on both a and α_2, its sign depending on the competition between viscous heating and inelastic cooling. If viscous heating dominates (i.e., $\eta_2^* a^2 > d\zeta_2^*/2$), then $\gamma > 0$. On the other hand, $\gamma < 0$ in the opposite situation (i.e., $\eta_2^* a^2 < d\zeta_2^*/2$). The two effects cancel each other (and thus $\gamma = 0$) at a threshold shear rate a_{th} given by

$$a_{\text{th}}^2 = \frac{d}{2}\frac{\zeta_2^*}{\eta_2^*(a_{\text{th}})}. \tag{2.28}$$

Since $\gamma = 0$ at $a = a_{\text{th}}$, it follows from equations (2.16) and (2.21) that $\nu_i^{-1}\partial_y T_i = \text{const}$. This condition, together with $n_i T_i = \text{const}$ and equations (2.24) and (2.25), implies that the heat flux is uniform at $a = a_{\text{th}}$ [41, 42, 50] for both the impurity and the host gas.

2.2. The kinetic model description of the Couette flow for the granular gas and the impurity

The mathematical complexity of the Boltzmann and Boltzmann–Lorentz equations (2.1) and (2.2) prevents one from obtaining exact solutions. This has motivated the proposal of simpler kinetic models, most of them inspired on the well-known Bhatnagar–Gross–Krook (BGK) kinetic model for ordinary gases [51]. Here we consider the following BGK-type kinetic model [35, 52]:

$$J_{i2}[\mathbf{v}|f_i, f_2] \to -k_d\frac{1+\alpha_i}{2}\nu_i\left(f_i - f_{i2}\right) + \frac{\zeta_i}{2}\frac{\partial}{\partial \mathbf{v}}\cdot\left[\left(\mathbf{v}-\mathbf{u}_i\right)f_i\right], \tag{2.29}$$

where

$$f_{i2}(\mathbf{v}) = n_i\left(\frac{m_i}{2\pi T_{i2}}\right)^{d/2}\exp\left[-\frac{m_i}{2T_{i2}}\left(\mathbf{v}-\mathbf{u}_{i2}\right)^2\right] \tag{2.30}$$

is a reference distribution function. In the case of the granular gas ($i = 2$), $T_{22} = T_2$ and $\mathbf{u}_{22} = \mathbf{u}_2$, so f_{22} is the local equilibrium distribution function. In the case of the impurity particles ($i = 1$) [35],

$$T_{12} = T_1 + \frac{2\mu}{(1+\mu)^2}\left\{T_2 - T_1 + \frac{(\mathbf{u}_1-\mathbf{u}_2)^2}{2d}\left[m_2 + \frac{T_2-T_1}{T_1/m_1 + T_2/m_2}\right]\right\}, \tag{2.31}$$

$$\mathbf{u}_{12} = \frac{\mu\mathbf{u}_1 + \mathbf{u}_2}{1+\mu}, \tag{2.32}$$

where

$$\mu \equiv \frac{m_1}{m_2} \tag{2.33}$$

is the mass ratio. In equation (2.29)

$$\zeta_2 = \frac{d+2}{4d}(1-\alpha_2^2)\nu_2 \tag{2.34}$$

is the cooling rate (2.11) evaluated in the local equilibrium approximation, while

$$\zeta_1 = \frac{d+2}{2d}\frac{\nu_1}{(1+\mu)^2}\left[1 + \frac{m_1 T_2}{m_2 T_1} + \frac{3}{2d}\frac{m_1}{T_1}(\mathbf{u}_1-\mathbf{u}_2)^2\right](1-\alpha_1^2) \tag{2.35}$$

J. Stat. Mech. (2011) P07005

is the impurity cooling rate. Finally, the factor k_d can be chosen to optimize agreement with the Boltzmann description. In particular, the choices $k_d = 1$ and $k_d = Pr = (d-1)/d$ reproduce the NS shear viscosity and thermal conductivity coefficients, respectively, of the gas in the elastic limit [18, 51]. A third criterion for fixing the factor k_d is to require that the collisional momentum transfer of the impurities be the same for the kinetic model as for the true Boltzmann–Lorentz equation [35, 36]. This results in $k_d = (d+2)/d$.

In a recent work [36], we solved the kinetic model equations for the granular gas and impurity in the steady Couette flow. The resulting profiles agree with the forms (2.14)–(2.16) and (2.19)–(2.21). Moreover, the solution gives γ, χ, η_1^*, $\theta_{1,x}$, $\theta_{1,y}$, λ_1^*, and ϕ_1^* as functions of a, α_1, α_2, μ, and $\omega \equiv \sigma_1/\sigma_2$. Their explicit forms are displayed in the appendix.

2.3. Numerical methods (Monte Carlo simulations)

As we said in section 1, we have solved numerically the Boltzmann and Boltzmann–Lorentz kinetic equations for the hard-sphere ($d = 3$) granular gas and impurity (equations (2.1) and (2.2), respectively) by means of the DSMC method. Originally devised for elastic gases in the low density limit [43], this method has been successfully implemented also for inelastic hard spheres [41] and moderately dense gases (the Enskog kinetic equation [53]–[55]).

The implementation of the algorithm for granular gases has been described in more detail elsewhere (see, for instance, [42]). We will recall only that it consists of small time steps (on the scale of the characteristic mean free time), each one having two basic stages: (i) free streaming and (ii) stochastic interparticle (binary) collisions. The system is divided into small cells (on the scale of the characteristic mean free path). In the DSMC method, the number N_i of simulated particles is a statistical technical parameter that, in contrast to the molecular dynamics case, does not need to coincide with the actual number of physical particles in the system. We have used the same number of simulated particles ($N_1 = N_2 = 2 \times 10^5$) for both species. On the other hand, since the physical impurity concentration is assumed to be negligibly small, only 2–2 collisions are considered in the evolution of the granular gas and only 1–2 collisions are considered in the evolution of the impurity particles. Therefore, after a collision of type 2–2, the velocities of both particles are changed, while only the velocity of the impurity particle is changed after a collision of type 1–2.

As in a previous work [42], we perform two averages for steady states: (i) a first spatial average over neighbor simulation cells, taking care that this coarse-grained cell size is not larger than the typical length over which hydrodynamic fields vary, and (ii) a time average for each coarse-grained cell since the microstates of the simulation are stored iteratively many times during the stationary state in the simulation.

Since the parameter space (mass ratio $\mu \equiv m_1/m_2$, size ratio $\omega \equiv \sigma_1/\sigma_2$, coefficients of restitution α_1 and α_2, and shear rate a) is quite large, we have focused on a few representative cases. As in our previous work on the BGK-type model [36], we have analyzed cases with a common coefficient of restitution ($\alpha_1 = \alpha_2 = \alpha$) and equal diameter ($\omega = 1$) for $d = 3$ (spheres). Three different values of the mass ratio ($\mu = 2, 1, 0.5$) and of the coefficient of restitution ($\alpha = 1, 0.9, 0.8$) have been considered. Thus, the elastic limit ($\alpha = 1$) as well as the properties of the granular gas ($\mu = 1$) are included

J. Stat. Mech. (2011) P07005

as particular cases. For each one of the nine combinations of the pair (μ, α), we have made series of simulations in shear rate a by keeping fixed the wall velocity difference $U = 10$, but varying the wall distance in the range $L = 2.5$–30. We will use hereafter nondimensionalized quantities with the following choice of units: $m_2 = 1$, $T_2(\pm L/2) = 1$, and $\nu_2(\pm L/2) = 1$. Also, we define the density levels $\bar{n}_i = 1$, where the bar denotes a spatial average across the system.

In section 3 we compare the DSMC numerical solution of the Boltzmann description with the analytical solution of the BGK-type kinetic model. But, before that, it is appropriate to show DSMC data confirming that the hypotheses on which our theoretical description relies (equations (2.14), (2.15), (2.18)–(2.21)) are indeed valid. As an illustration, figures 2 and 3 display the DSMC profiles for the cases $(\mu, \alpha) = (2, 0.9)$ and $(\mu, \alpha) = (0.5, 0.8)$. From figure 2 we observe that the hydrostatic pressure p_2 of the granular gas, except for small inflections near the boundary layers, is flat, the local shear rate a is indeed constant throughout the system, and the temperature T_2 is a linear function of $u_{2,x}^2$. Figure 3 confirms the remaining hypotheses (2.19)–(2.21), specific to the granular impurity. The 'enslaving' condition $\mathbf{u}_1 = \mathbf{u}_2$ is fulfilled with a very high degree of accuracy for all points in the system, even in the boundary layers. Moreover, the relative impurity concentration and the temperature ratio are practically constant.

3. Results and discussion

3.1. The threshold shear rate

We first consider the threshold value of the shear rate $a_{\rm th}$ at which the thermal curvature parameter γ vanishes. As discussed below equation (2.27), the value $a = a_{\rm th}$ is especially important since it corresponds to an exact balance between viscous heating and inelastic cooling, giving rise to $\mathbf{q}_i = \text{const}$. In the geometry sketched in figure 1, where the two walls are maintained at the same temperature, the value $\gamma = 0$ implies a constant temperature T_2 and thus the Couette flow becomes equivalent to the well-known simple shear flow [31]–[33]. More generally, when the walls are allowed to have different temperatures ($\Delta T = T_{\rm w+}/T_{\rm w-} - 1 \neq 0$), the limit case $\gamma = 0$ defines, in the parameter space $\{\alpha, a, \Delta T\}$, a surface that has been shown recently [41, 42] to represent a special class of granular flows, including the conventional Fourier flow of an elastic gas. This generalized class of flows (that we called 'LTu' because the temperature is a linear function of the flow velocity) can be theoretically described in a single hydrodynamic theory frame, both for elastic and for granular gases.

Figure 4 shows the α-dependence of the threshold shear rate $a_{\rm th}$, as predicted by the BGK-type kinetic model, equation (A.10), with the three choices of k_d mentioned before, namely $k_d = 1$, $k_d = (d-1)/d$, and $k_d = (d+2)/d$. The simulation data obtained here for $\alpha = 0.8$ and 0.9 with $\Delta T = 0$, as well as those of [42] for a wider range with $\Delta T \neq 0$, are also included in figure 4. We clearly observe that the best agreement is achieved with the choice $k_d = 1$. Although we have checked that either $k_d = (d-1)/d$ or $k_d = (d+2)/d$ may provide a better agreement with simulation for some of the other quantities, henceforth we will adopt the choice $k_d = 1$ as a convenient compromise between simplicity and accuracy.

In the rest of this section, we will compare DSMC results from the Boltzmann equation with the analytical results derived from our BGK-type model, representing the relevant

J. Stat. Mech. (2011) P07005

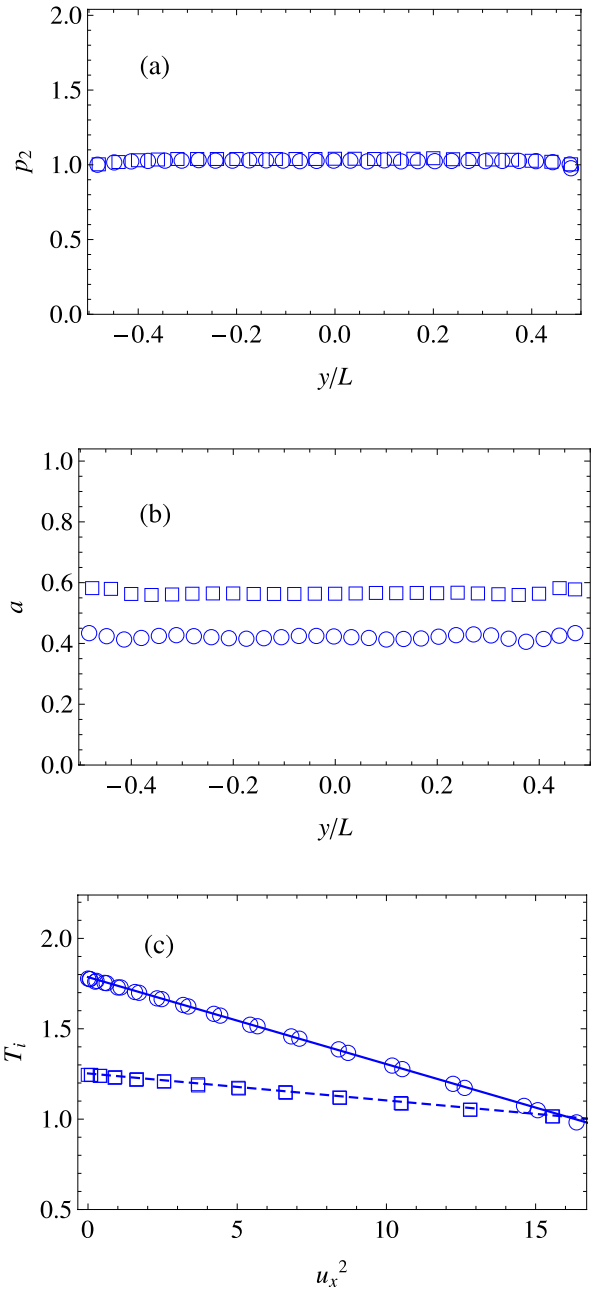

Figure 2. This figure illustrates the verification in the bulk region of the three hypotheses on the stationary Couette flow for the granular gas: (a) the hydrostatic pressure p_2 is constant, (b) the local shear rate a is also constant, and (c) the temperature T_2 is a linear function of $u_{2,x}^2$. Two values of the coefficient of restitution are considered: $\alpha_2 = 0.9$ (○ , with $L = 23.23$ and $a = 0.443$) and $\alpha_2 = 0.8$ (□, with $L = 15.48$ and $a = 0.571$). Lines in (c) stand for linear fits to DSMC data.

J. Stat. Mech. (2011) P07005

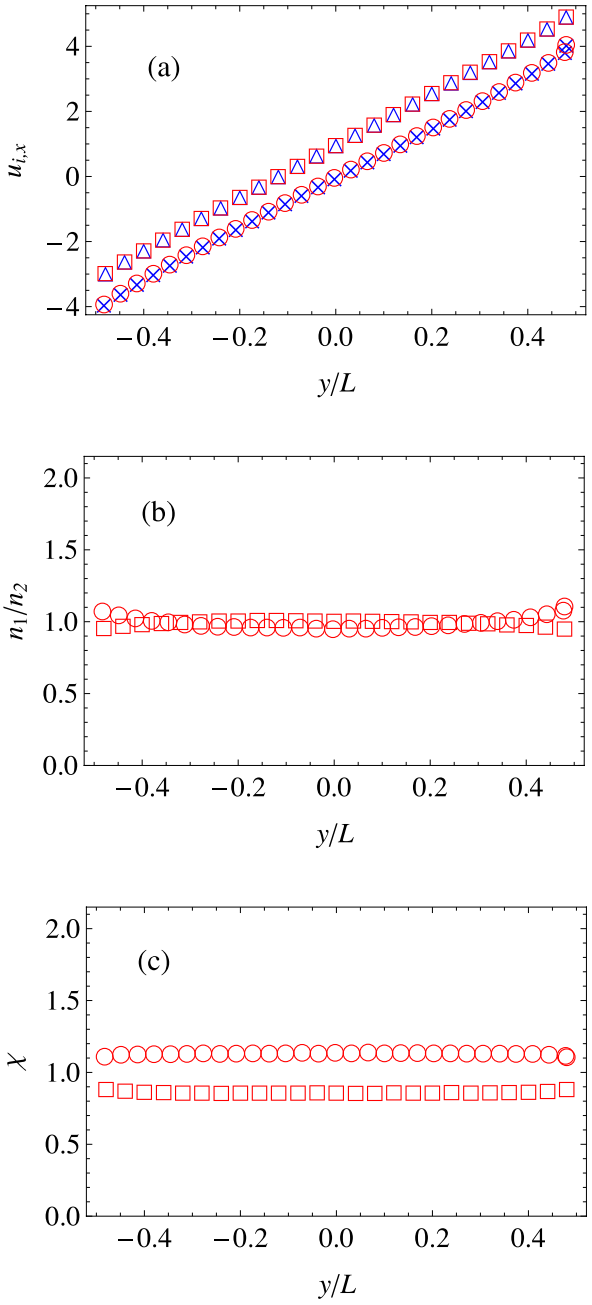

Figure 3. This figure illustrates the verification in the bulk region of the three hypotheses on the stationary Couette flow for the impurity: (a) no mutual diffusion exists, i.e., $u_{1,x}(y) = u_{2,x}(y)$, (b) the mole fraction n_1/n_2 is constant, and (c) the temperature ratio $\chi = T_1/T_2$ is also constant. Two cases are considered: $\alpha_1 = \alpha_2 = 0.9$, $\mu = 2$, $\omega = 1$ (○, with $L = 23.23$ and $a = 0.443$) and $\alpha_1 = \alpha_2 = 0.8$, $\mu = 0.5$, $\omega = 1$ (□, with $L = 15.48$ and $a = 0.571$). In panel (a) the crosses and triangles correspond to the granular gas ($i = 2$), and the symbols corresponding to $\alpha = 0.8$ have been lifted to avoid overlap with the symbols corresponding to $\alpha = 0.9$. In panel (b) the density n_i is normalized with respect to its spatial average value $\bar{n}_i$.

J. Stat. Mech. (2011) P07005

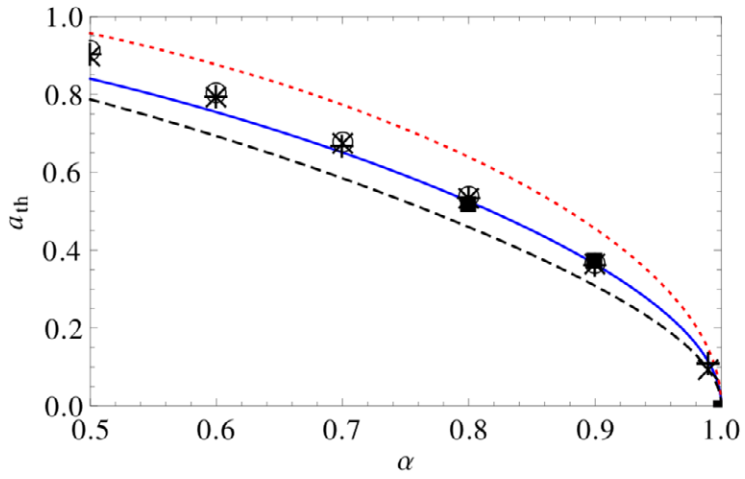

Figure 4. Threshold values $a_{\rm th}$ for the shear rate a versus the coefficient of normal restitution for spheres ($d = 3$). The lines represent the theoretical results given by equation (A.10) with three different choices for the parameter k_d: $k_d = 1$ (solid line), $k_d = Pr = (d-1)/d$ (dashed line), and $k_d = (d+2)/d$ (dotted line). Symbols stand for DSMC simulation data with $\Delta T = 0$ (■, this work), $\Delta T = 2$ (×, [41, 42]), $\Delta T = 10$ (+, [41, 42]), and simple shear flow (○ , [56]).

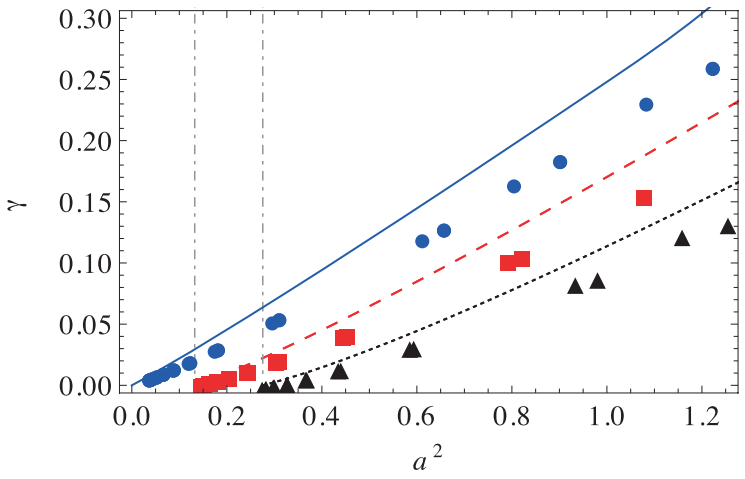

Figure 5. Thermal curvature coefficient γ as a function of the square of the shear rate, a^2. From now on, in all figures, lines stand for the BGK-type theory (with $k_d = 1$) and symbols stand for DSMC data. Three series are plotted: $\alpha = 1$ (solid line and circles), $\alpha = 0.9$ (dashed line and squares), and $\alpha = 0.8$ (dotted line and triangles). The threshold levels $a_{\rm th}^2$ for the shear rate in the cases $\alpha = 0.9$ and $\alpha = 0.8$ are marked with dotted–dashed vertical lines.

hydrodynamic properties as functions of the shear rate (for $a \geq a_{\rm th}$), so we can analyze to what extent the nonlinear theoretical description is reliable, at least at a qualitative level, for these very far away from equilibrium steady states.

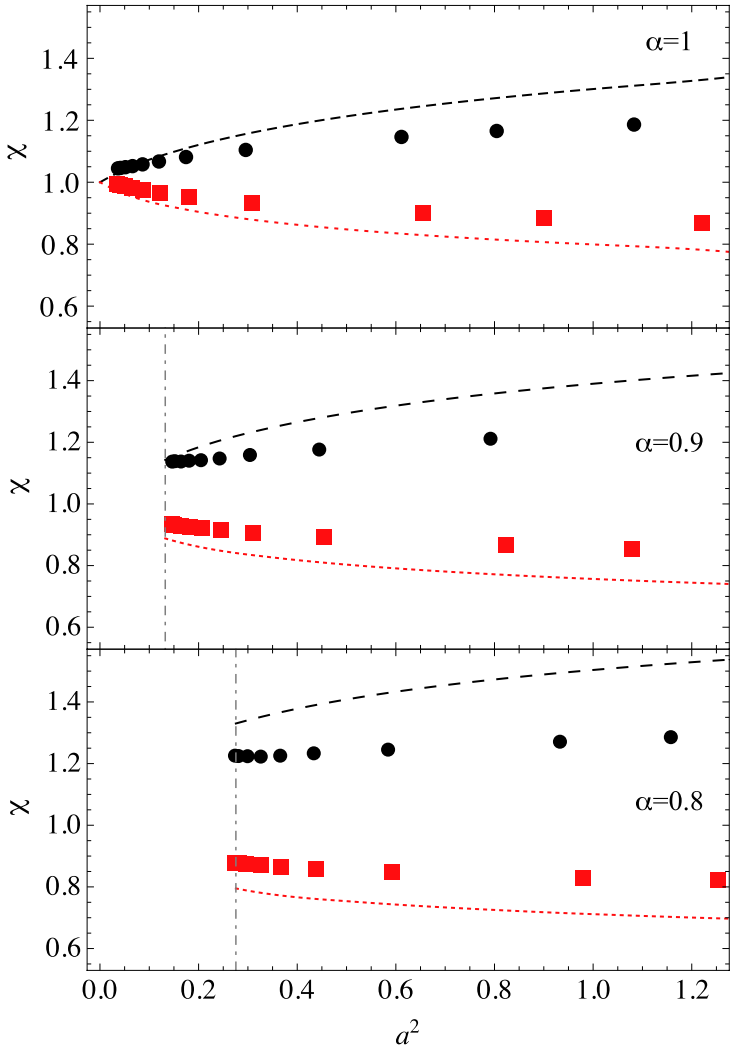

Figure 6. Temperature ratio $\chi \equiv T_1/T_2$ as a function of the square of the shear rate, a^2. Two mass ratios are considered for each value of α: $\mu \equiv m_1/m_2 = 2$ (dashed lines and circles) and $\mu = 1/2$ (dotted lines and squares). The threshold levels $a_{\rm th}^2$ for the shear rate in the cases $\alpha = 0.9$ and $\alpha = 0.8$ are marked with dotted–dashed vertical lines.

3.2. Thermal curvature coefficient γ and temperature ratio χ

In figure 5 we can see that the theoretical thermal curvature parameter shows a good agreement with DSMC data. The agreement is quantitatively very good near the threshold $a_{\rm th}$, but the theory tends to overestimate γ as the shear rate increases. In any case, we can observe in figure 5 the reliability of our non-Newtonian hydrodynamic description in the context of the BGK-type kinetic model. As usual, the thermal curvature parameter decreases for decreasing shear rate, until it reaches a threshold value $\gamma = 0$ at which we obtain the simple shear flow [33] or, more generally, the LTu class flow [41, 42, 50]. We should recall that the BGK solution is not mathematically well defined for states with $\gamma < 0$ (see, however, [57] for an analytical continuation). In principle, it should be also

J. Stat. Mech. (2011) P07005

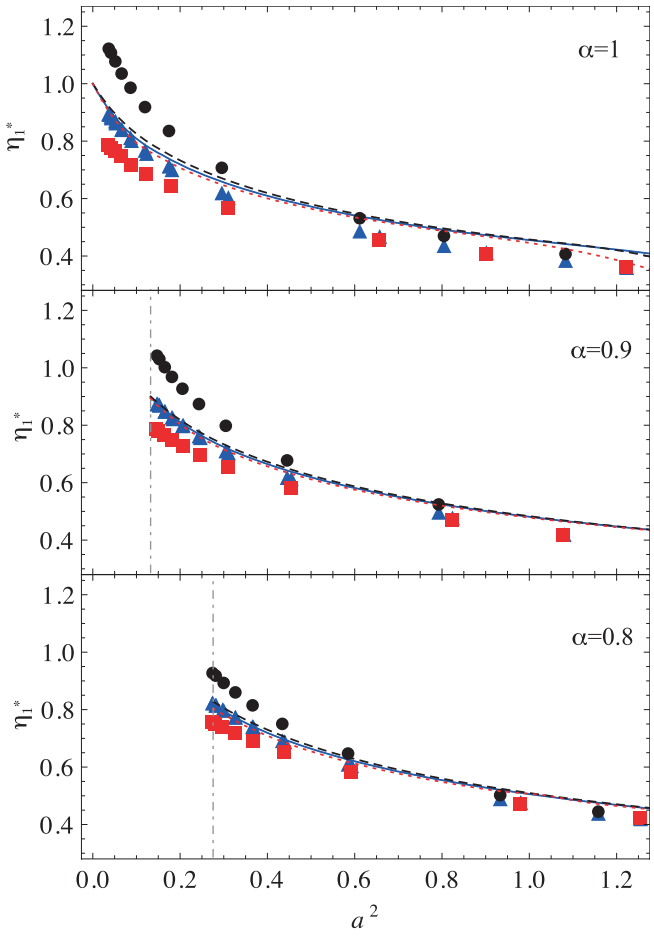

Figure 7. Reduced shear viscosity η_1^* as a function of the square of the shear rate, a^2. Three mass ratios are considered for each value of α: $\mu \equiv m_1/m_2 = 2$ (dashed lines and circles), $\mu = 1$ (solid lines and triangles), and $\mu = 1/2$ (dotted lines and squares). The threshold levels a_{th}^2 for the shear rate in the cases $\alpha = 0.9$ and $\alpha = 0.8$ are marked with dotted–dashed vertical lines.

possible to find nonlinear Couette flows from the Boltzmann equation (it has already been shown that these states do exist in the quasielastic limit [30]). This region would correspond to points below the LTu surface [41, 42].

In figure 6 we plot the results for the temperature ratio. We may confirm that the Boltzmann equation solution follows the same general trends as the BGK-type model [36]. In particular, the impurity has a higher (lower) temperature than the granular gas if its mass is larger (smaller) than that of a gas particle, this effect being more pronounced as the shear rate increases. On the other hand, the BGK-type model tends to exaggerate these effects.

3.3. Generalized transport coefficients

In figure 7 we present the results for the shear viscosity η_1^*. As we can observe, the kinetic model predicts that η_1^* is practically independent of the mass ratio μ. This feature is also

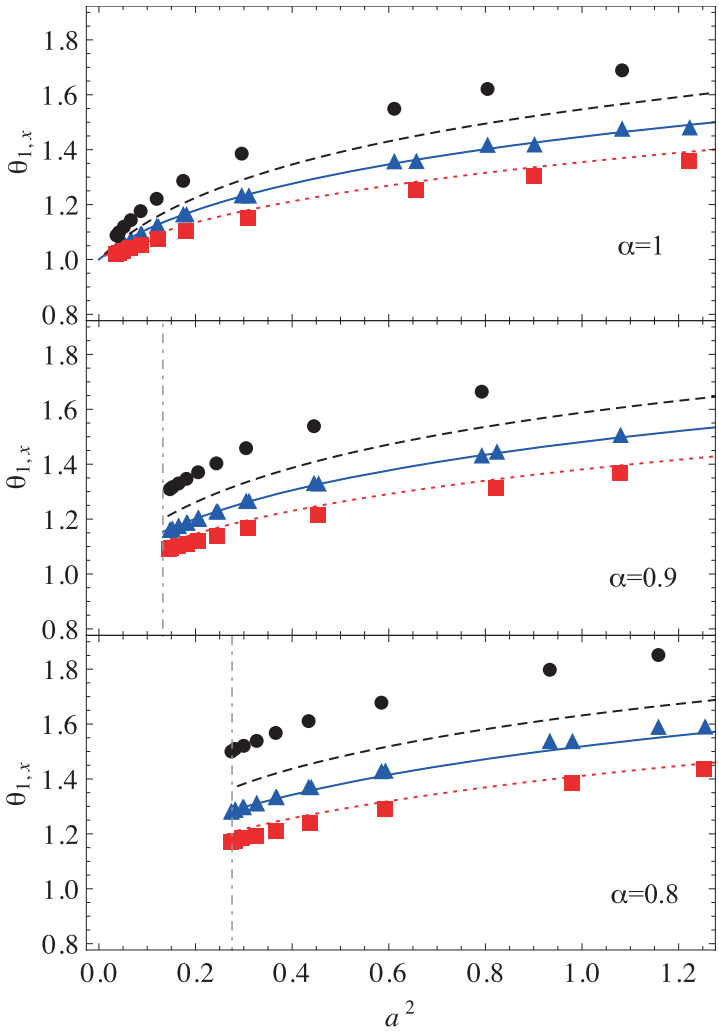

Figure 8. Normal stress coefficient $\theta_{1,x}$ as a function of the square of the shear rate, a^2. Three mass ratios are considered for each value of α: $\mu \equiv m_1/m_2 = 2$ (dashed lines and circles), $\mu = 1$ (solid lines and triangles), and $\mu = 1/2$ (dotted lines and squares). The threshold levels a_{th}^2 for the shear rate in the cases $\alpha = 0.9$ and $\alpha = 0.8$ are marked with dotted–dashed vertical lines.

shared by the DSMC data, except near a_{th}, where the values of η_1^* increase with the mass ratio. Apart from this, the kinetic model not only successfully captures the decrease of the shear viscosity with increasing shear rate (shear thinning), but also exhibits a generally good quantitative agreement.

The normal stress coefficients $\theta_{1,x}$ and $\theta_{1,y}$ are displayed in figures 8 and 9, respectively. While $\theta_{1,x} > 1$, we observe that $\theta_{1,y} < 1$, this anisotropic effect increasing with increasing shear rate, with increasing mass ratio, and with increasing collisional dissipation. The kinetic model correctly accounts for these trends. At a quantitative level, the agreement is fairly good for $\mu \leq 1$ (especially in the case of $\theta_{1,x}$). However, in the case of heavy impurities ($\mu > 1$), the kinetic model clearly underestimates the deviations of $\theta_{1,x}$ and $\theta_{1,y}$ from unity.

J. Stat. Mech. (2011) P07005

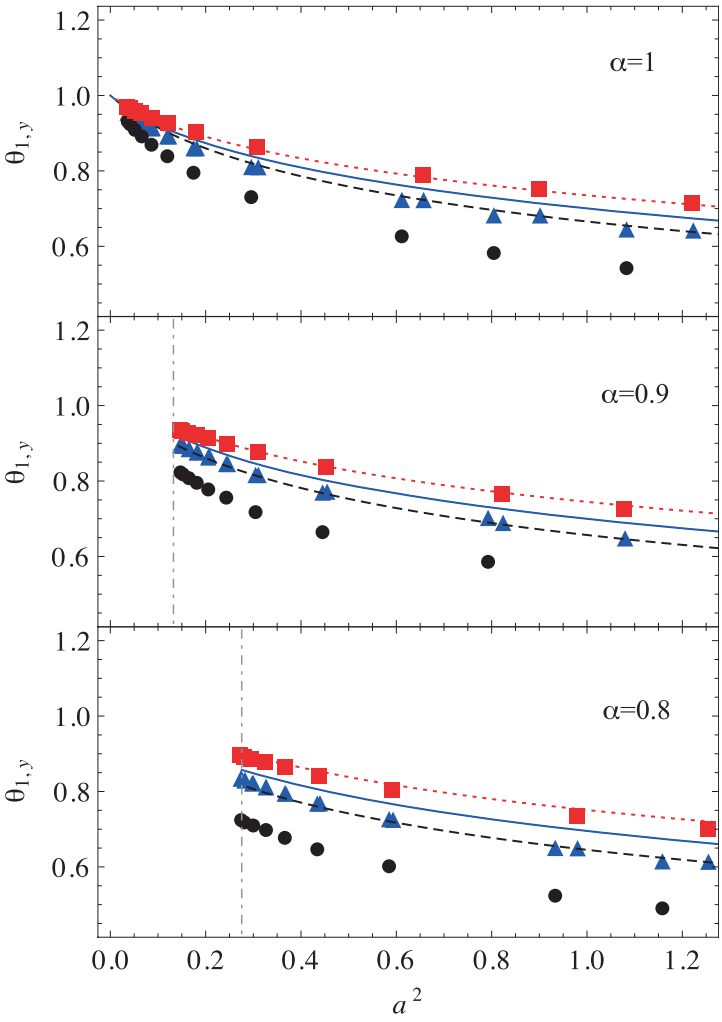

Figure 9. Normal stress coefficient $\theta_{1,y}$ as a function of the square of the shear rate, a^2. Three mass ratios are considered for each value of α: $\mu \equiv m_1/m_2 = 2$ (dashed lines and circles), $\mu = 1$ (solid lines and triangles), and $\mu = 1/2$ (dotted lines and squares). The threshold levels $a_{\rm th}^2$ for the shear rate in the cases $\alpha = 0.9$ and $\alpha = 0.8$ are marked with dotted–dashed vertical lines.

The heat flux transport coefficients λ_1^* and ϕ_1^* are shown in figures 10 and 11, respectively. The theoretical curves for λ_1^* and, especially, for ϕ_1^* are more sensitive to the value of the mass ratio μ than those for η_1^*, showing that the heat flux transport coefficients increase with increasing μ. These features are generally confirmed by the DSMC data for ϕ_1^* but in the case of λ_1^* the influence of μ is less clear, except near the threshold shear rate. Apart from that, the kinetic model correctly describes the decrease of λ_1^* with increasing shear rate as well as the change in the dependence of ϕ_1^* on a as one goes from the elastic case ($\alpha = 1$) to the inelastic ones ($\alpha = 0.9$ and 0.8). It is interesting to remark that the cross thermal conductivity coefficient ϕ_1^* (an obvious non-Newtonian effect) can become larger than the generalized NS thermal conductivity coefficient λ_1^*. This effect was already observed in the special case of LTu flows in one-

J. Stat. Mech. (2011) P07005

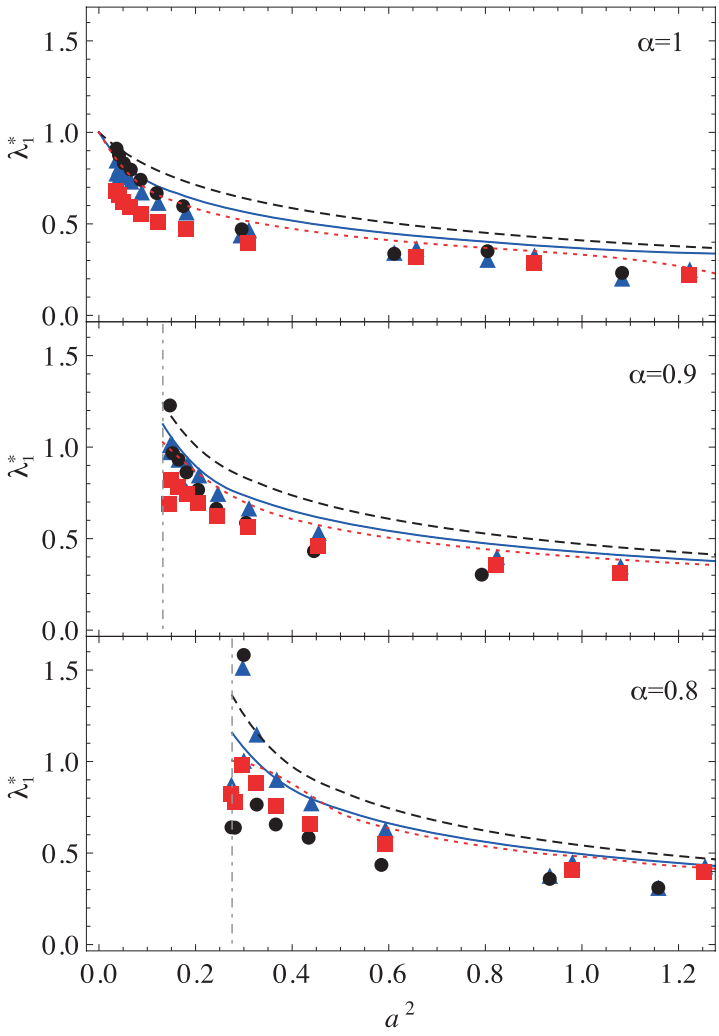

Figure 10. Reduced thermal conductivity λ_1^* as a function of the square of the shear rate, a^2. Three mass ratios are considered for each value of α: $\mu \equiv m_1/m_2 = 2$ (dashed lines and circles), $\mu = 1$ (solid lines and triangles), and $\mu = 1/2$ (dotted lines and squares). The threshold levels a_{th}^2 for the shear rate in the cases $\alpha = 0.9$ and $\alpha = 0.8$ are marked with dotted–dashed vertical lines.

component systems [41, 42]. Now, both the kinetic model and the DSMC data show that the inequality $\phi_1^* > \lambda_1^*$ (i.e., $|q_{1,x}| > |q_{1,y}|$) becomes more pronounced as the shear rate or the mass ratio increases.

4. Conclusions

We have analyzed in this paper the properties of the Couette flow for a granular impurity immersed in a granular gas. We have focused on the region of high shear rates, i.e., $a > a_{\text{th}}$, where viscous heating prevails over inelastic cooling and thus the thermal curvature coefficient γ defined by equation (2.16) is positive. This corresponds to states in

J. Stat. Mech. (2011) P07005

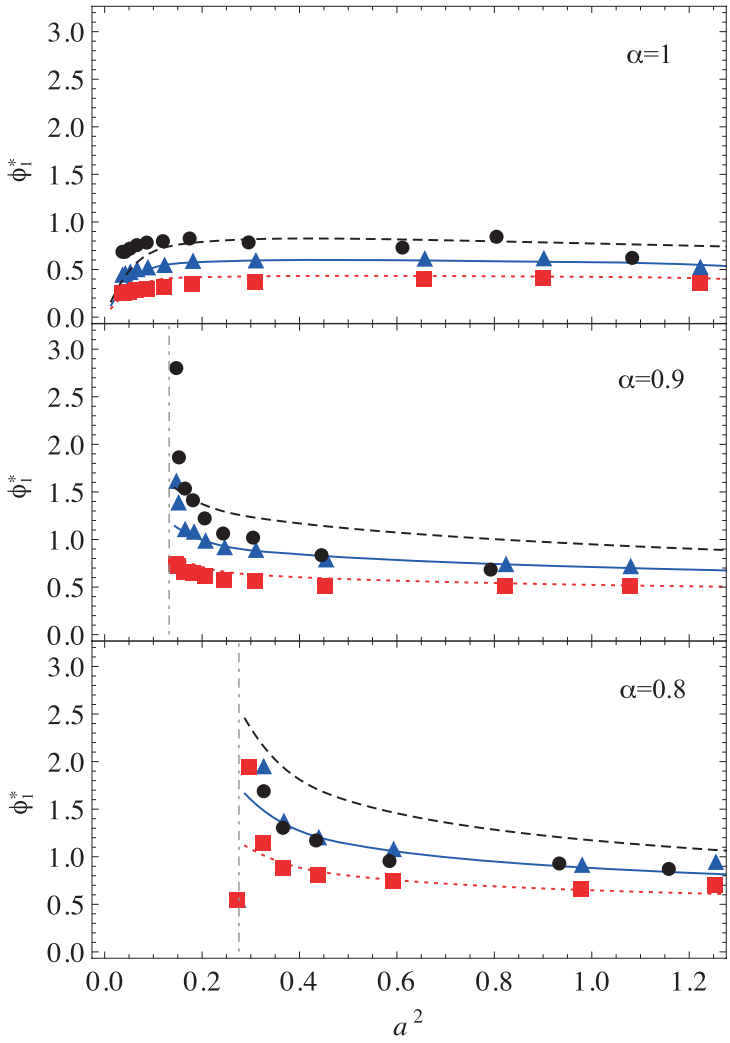

Figure 11. Reduced cross thermal conductivity ϕ_1^* as a function of the square of the shear rate, a^2. Three mass ratios are considered for each value of α: $\mu \equiv m_1/m_2 = 2$ (dashed lines and circles), $\mu = 1$ (solid lines and triangles), and $\mu = 1/2$ (dotted lines and squares). The threshold levels a_{th}^2 for the shear rate in the cases $\alpha = 0.9$ and 0.8 are marked with dotted–dashed vertical lines.

the region above the LTu surface described in a previous work [41, 42], where an analytical solution from a BGK-type model is available [36] and, more importantly, nonlinear effects are dominant. We have confirmed that the hypotheses made in order to obtain the BGK-type theoretical solution in a previous work [36, 46] also apply for the numerical solution of the inelastic Boltzmann and Boltzmann–Lorentz equations: (i) the pressure p_2 of the granular gas is uniform, (ii) the local shear rate $\partial u_{2,x}/\partial y$ divided by the local collision frequency $\nu_2 \propto n_2 T_2^{1/2}$ is uniform, (iii) the temperature T_2 of the granular gas is a quadratic function of the flow velocity $u_{2,x}$, (iv) the flow velocity of the impurity coincides with that of the gas, i.e., $u_{1,x} = u_{2,x}$, (v) the mole fraction n_1/n_2 of the impurity is uniform, and (vi) the impurity/gas temperature ratio $\chi \equiv T_1/T_2$ is also uniform. The fourth hypothesis on the absence of mutual diffusion is fulfilled with an especially high

J. Stat. Mech. (2011) P07005

degree of accuracy, since we were unable to measure any non-negligible difference between the profiles $\mathbf{u}_{1,x}(y)$ and $\mathbf{u}_{2,x}(y)$ over a wide range of situations (see figure 3(a) for reference). This is important since it delimits well the properties of the Couette flow for the impurity, which has important consequences in applications such as segregation [15].

Apart from the validation of the hydrodynamic hypotheses (i)–(vi), the DSMC results have shown a good semi-quantitative validity of the theoretical predictions as regards the dependence of non-Newtonian properties (temperature ratio, normal stress differences, generalized shear viscosity, and generalized thermal conductivities) on the shear rate, the mass ratio, and the coefficient of restitution.

Although we have limited our study to the region $a > a_{\text{th}}$ (i.e., $\gamma > 0$), preliminary results seem to indicate that the special LTu state ($a = a_{\text{th}}$ or $\gamma = 0$) also exists for the granular impurity (and exactly at the same point as occurs for the granular gas). This, together with the fact that the impurity in any case fulfills also the hypotheses (i)–(iii) for the granular gas, suggests that we can perform a classification of Couette flows for the impurity analogous to that for the granular gas [30, 41]. Therefore, an interesting way in which our work can be extended consists of studying Couette flows for non-equal temperature walls and in the region below a_{th}. Theoretical and numerical work on this subject is ongoing.

Acknowledgments

This research was supported by the Ministerio de Ciencia e Innovación (Spain) through Grants No. FIS2010-16587 and (only FVR) No. MAT2009-14351-C02-02, partially financed by FEDER funds. Support from the Junta de Extremadura (Spain) through Grant No. GR10158 is also gratefully acknowledged.

Appendix. Transport properties of the impurity from the BGK-type kinetic model

We present in this appendix the explicit expressions for the relevant hydrodynamic properties, as extracted from a previous work [36]. Those expressions are given in terms of some mathematical functions that we define below.

First, we introduce the functions

$$F_{0,m}(y,z) \equiv \int_0^\infty \mathrm{d}w\, \mathrm{e}^{-(1+z)w} w^m X_0\left(\Theta(w,y,z)\right), \tag{A.1}$$

$$\begin{aligned} F_{1,m}(y,z) &\equiv y\frac{\partial}{\partial y} F_{0,m}(y,z) \\ &= -\frac{1}{2}\int_0^\infty \mathrm{d}w\, \mathrm{e}^{-(1+z)w} w^m \frac{X_1\left(\Theta(w,y,z)\right)}{\Theta(w,y,z)} \end{aligned} \tag{A.2}$$

where

$$X_0(\Theta) \equiv \sqrt{\pi}\Theta\, \mathrm{e}^{\Theta^2}\mathrm{erfc}(\Theta) - 1, \qquad X_1(\Theta) \equiv \Theta^2\left[\sqrt{\pi}(1+2\Theta^2)\mathrm{e}^{\Theta^2}\mathrm{erfc}(\Theta) - 2\Theta\right], \tag{A.3}$$

$$\Theta(w,y,z) \equiv \frac{1}{2\sqrt{2y}}\frac{z}{1-\mathrm{e}^{-(1/2)zw}}. \tag{A.4}$$

J. Stat. Mech. (2011) P07005

In equation (A.3), $\mathrm{erfc}(x)$ is the complementary error function. Note that, because of the square root in equation (A.4), the functions $F_{0,m}(y,z)$ and $F_{1,m}(y,z)$ are only well defined for $y \geq 0$. Next, we define

$$G(y,z) \equiv \int_0^\infty \mathrm{d}w\, \mathrm{e}^{-(1+(3/2)z)w} w \left[\frac{d+1}{2} X_1(\Theta(w,y,z)) + Y(\Theta(w,y,z))\right], \tag{A.5}$$

$$H(y,z) \equiv \int_0^\infty \mathrm{d}w\, \mathrm{e}^{-(1+(3/2)z)w} w^3 Y(\Theta(w,y,z)), \tag{A.6}$$

where

$$Y(\Theta) \equiv \Theta^3[2(1+\Theta^2) - \sqrt{\pi}\Theta(3+2\Theta^2)\mathrm{e}^{\Theta^2}\mathrm{erfc}(\Theta)]. \tag{A.7}$$

Now that we have introduced the above functions, let us display the expressions for the solution of the kinetic model. First, the thermal curvature coefficient γ is given as a function of the reduced shear rate a and the coefficient of restitution α_2 through the implicit equation

$$\begin{aligned} d\frac{c_2\zeta_2^*}{1+c_2\zeta_2^*} - \frac{2c_2^2a^2}{(1+c_2\zeta_2^*)^3} &= 2F_{1,0}(c_2^2\gamma, c_2\zeta_2^*) + dF_{0,0}(c_2^2\gamma, c_2\zeta_2^*) \\ &+ c_2^2a^2\left[2F_{1,2}(c_2^2\gamma, c_2\zeta_2^*) + F_{0,2}(c_2^2\gamma, c_2\zeta_2^*)\right], \end{aligned} \tag{A.8}$$

where

$$c_i \equiv \frac{2}{k_d(1+\alpha_i)}. \tag{A.9}$$

Since the functions (A.1) and (A.2) are not defined for negative y, the representation (A.8) exists only for $\gamma \geq 0$ or, equivalently, for $a \geq a_{\mathrm{th}}$, where the threshold value a_{th} of the shear rate (corresponding to $\gamma = 0$) is [36, 46]

$$a_{\mathrm{th}}^2 = \frac{d}{2c_2}\zeta_2^*(1+c_2\zeta_2^*)^2. \tag{A.10}$$

In the case $a = a_{\mathrm{th}}$ the viscous heating is exactly balanced by collisional cooling and the heat flux becomes uniform [41, 42, 50].

Next, the temperature ratio $\chi = T_1/T_2$ is obtained from the implicit equation

$$\begin{aligned} d\left(\frac{T_1}{T_{12}} - \frac{1}{1+\tilde{\zeta}_1}\right) - \frac{2\tilde{a}^2}{(1+\tilde{\zeta}_1)^3} &= 2F_{1,0}(\tilde{\gamma}, \tilde{\zeta}_1) + dF_{0,0}(\tilde{\gamma}, \tilde{\zeta}_1) \\ &+ \tilde{a}^2\left[2F_{1,2}(\tilde{\gamma}, \tilde{\zeta}_1) + F_{0,2}(\tilde{\gamma}, \tilde{\zeta}_1)\right]. \end{aligned} \tag{A.11}$$

Here,

$$\tilde{a} \equiv \frac{\nu_2}{\nu_1}c_1 a, \qquad \tilde{\gamma} \equiv \frac{\nu_2^2}{\nu_1^2}\frac{T_{12}}{T_1}\frac{\chi}{\mu}c_1^2\gamma, \tag{A.12}$$

$$\tilde{\zeta}_1 \equiv \frac{c_1\zeta_1}{\nu_1} = c_1\frac{d+2}{2d}\frac{\mu+\chi}{(1+\mu)^2\chi}(1-\alpha_1^2). \tag{A.13}$$

In equation (A.13) use has been made of equation (2.35) with $\mathbf{u}_1 = \mathbf{u}_2$. Moreover, from

J. Stat. Mech. (2011) P07005

equations (2.17), (2.26), and (2.31), we have

$$\frac{\nu_2}{\nu_1}=\left(\frac{2}{1+\omega}\right)^{d-1}\sqrt{\frac{2\mu}{\mu+\chi}},\qquad \frac{T_{12}}{T_1}=1+\frac{2\mu(1-\chi)}{(1+\mu)^2\chi}. \tag{A.14}$$

We recall that $\omega\equiv\sigma_1/\sigma_2$.

Finally, the transport coefficients defined by equations (2.22)–(2.25) are

$$\eta_1^*=c_1\frac{T_{12}}{T_1}\left[\frac{1}{(1+\tilde{\zeta}_1)^2}+F_{0,1}(\tilde{\gamma},\tilde{\zeta}_1)+2F_{1,1}(\tilde{\gamma},\tilde{\zeta}_1)\right], \tag{A.15}$$

$$\theta_{1,x}=d-\frac{T_{12}}{T_1}\left[\frac{d-1}{1+\tilde{\zeta}_1}+(d-1)F_{0,0}(\tilde{\gamma},\tilde{\zeta}_1)+2F_{1,0}(\tilde{\gamma},\tilde{\zeta}_1)\right], \tag{A.16}$$

$$\theta_{1,y}=\frac{T_{12}}{T_1}\left[\frac{1}{1+\tilde{\zeta}_1}+F_{0,0}(\tilde{\gamma},\tilde{\zeta}_1)+2F_{1,0}(\tilde{\gamma},\tilde{\zeta}_1)\right], \tag{A.17}$$

$$\lambda_1^*=\frac{1}{d+2}\frac{T_{12}}{T_1}\frac{1}{\tilde{\gamma}}\left[\eta_1^*\tilde{a}^2-c_1\frac{d}{2}\left(1-\frac{T_{12}}{T_1}+\tilde{\zeta}_1\right)\right], \tag{A.18}$$

$$\phi_1=\frac{2c_1}{d+2}\left(\frac{T_{12}}{T_1}\right)^2\frac{\tilde{a}}{\sqrt{2\tilde{\gamma}}}\left[G(\tilde{\gamma},\tilde{\zeta}_1)+\tilde{a}^2H(\tilde{\gamma},\tilde{\zeta}_1)\right], \tag{A.19}$$

where we have taken into account that $Pr=1$ in the BGK model [51].

The transport coefficients for the granular gas are easily deduced from equations (A.15)–(A.19) by making the formal replacements $1\to 2$, $\chi\to 1$, $\mu\to 1$, and $\omega\to 1$. It is then easy to check that equation (A.18) reduces to equation (2.27).

To conclude this appendix, let us write the results in the limit $a\to a_{\text{th}}$, i.e., $\gamma\to 0$. The temperature ratio is given by the physical root of the quartic equation [36]

$$d\left(\frac{T_1}{T_{12}}-\frac{1}{1+\tilde{\zeta}_1}\right)-\frac{2\tilde{a}_{\text{th}}^2}{(1+\tilde{\zeta}_1)^3}=0, \tag{A.20}$$

where $\tilde{a}_{\text{th}}$ is obtained from equations (A.10) and (A.12). Once χ is known, the transport coefficients are [36]

$$\eta_1^*=c_1\frac{T_{12}}{T_1}\frac{1}{(1+\tilde{\zeta}_1)^2}, \tag{A.21}$$

$$\theta_{1,x}=d-(d-1)\theta_{1,y},\qquad \theta_{1,y}=\frac{T_{12}}{T_1}\frac{1}{1+\tilde{\zeta}_1}, \tag{A.22}$$

$$\lambda_1^*=c_1\left(\frac{T_{12}}{T_1}\right)^2\frac{2}{2+7\tilde{\zeta}_1+6\tilde{\zeta}_1^2}\left[1+\frac{6}{d+2}\frac{12+42\tilde{\zeta}_1+37\tilde{\zeta}_1^2}{(2+7\tilde{\zeta}_1+6\tilde{\zeta}_1^2)^2}\tilde{a}_{\text{th}}^2\right], \tag{A.23}$$

$$\phi_1^*=c_1\frac{2}{d+2}\left(\frac{T_{12}}{T_1}\right)^2\frac{4+7\tilde{\zeta}_1}{(2+7\tilde{\zeta}_1+6\tilde{\zeta}_1^2)^2}\tilde{a}_{\text{th}}\left[d+4+18\frac{8+28\tilde{\zeta}_1+25\tilde{\zeta}_1^2}{(2+7\tilde{\zeta}_1+6\tilde{\zeta}_1^2)^2}\tilde{a}_{\text{th}}^2\right]. \tag{A.24}$$

Note that equations (A.10) and (A.21) (when the latter is particularized to the case of an impurity mechanically equivalent to the particles of the gas) are consistent with equation (2.28).

J. Stat. Mech. (2011) P07005

References

[1] Aranson I S and Tsimring L S, 2006 *Rev. Mod. Phys.* **78** 641
[2] Knight J B, Jaeger H M and Nagel S R, 1993 *Phys. Rev. Lett.* **70** 3728
[3] Jenkins J T and Yoon D K, 2002 *Phys. Rev. Lett.* **88** 194301
[4] Trujillo L, Alam M and Herrmann H J, 2003 *Europhys. Lett.* **64** 190
[5] Kudrolli A, 2004 *Rep. Prog. Phys.* **67** 209
[6] Brey J J, Ruiz-Montero M J and Moreno F, 2005 *Phys. Rev. Lett.* **95** 098001
[7] Brey J J, Ruiz-Montero M J and Moreno F, 2006 *Phys. Rev.* E **73** 031301
[8] Serero D, Goldhirsch I, Noskowicz S H and Tan M L, 2006 *J. Fluid Mech.* **554** 237
[9] Alam M, Trujillo L and Herrmann H J, 2006 *J. Stat. Phys.* **124** 587
[10] Garzó V, 2006 *Europhys. Lett.* **75** 521
[11] Melby P, Prevost A, Egolf D A and Urbach J S, 2007 *Phys. Rev.* E **76** 051307
[12] Garzó V, 2008 *Phys. Rev.* E **78** 020301(R)
[13] Garzó V, 2009 *Eur. Phys. J.* E **29** 261
[14] Serero D, Noskowicz S H, Tan M L and Goldhirsch I, 2009 *Eur. Phys. J. Spec. Top.* **179** 221
[15] Garzó V and Vega Reyes F, 2010 *J. Stat. Mech.* P07024
[16] Kudrolli A, 2010 *Phys. Rev. Lett.* **104** 088001
[17] Brey J J, Dufty J W, Kim C S and Santos A, 1998 *Phys. Rev.* E **58** 4638
[18] Chapman C and Cowling T G, 1970 *The Mathematical Theory of Non-Uniform Gases* 3rd edn (Cambridge: Cambridge University Press)
[19] Goldshtein A and Shapiro M, 1995 *J. Fluid Mech.* **282** 75
[20] Garzó V and Dufty J W, 2002 *Phys. Fluids* **14** 1476
[21] Garzó V, Vega Reyes F and Montanero J M, 2009 *J. Fluid Mech.* **623** 387
[22] Jenkins J T and Mancini F, 1987 *J. Appl. Mech.* **54** 27
[23] Jenkins J T and Mancini F, 1989 *Phys. Fluids* A **1** 2050
[24] Zamankhan P, 1995 *Phys. Rev.* E **52** 4877
[25] Arnarson B and Willits J T, 1998 *Phys. Fluids* **10** 1324
[26] Willits J T and Arnarson B, 1999 *Phys. Fluids* **11** 3116
[27] Garzó V, Dufty J W and Hrenya C M, 2007 *Phys. Rev.* E **76** 031303
[28] Garzó V, Hrenya C M and Dufty J W, 2007 *Phys. Rev.* E **76** 031304
[29] Garzó V and Vega Reyes F, 2009 *Phys. Rev.* E **79** 041303
[30] Vega Reyes F and Urbach J S, 2009 *J. Fluid Mech.* **636** 279
[31] Campbell C S, 1989 *J. Fluid Mech.* **203** 449
[32] Campbell C S, 1990 *Annu. Rev. Fluid Mech.* **22** 57
[33] Goldhirsch I, 2003 *Annu. Rev. Fluid Mech.* **35** 267
[34] Santos A, Garzó V and Dufty J W, 2004 *Phys. Rev.* E **69** 061303
[35] Vega Reyes F, Garzó V and Santos A, 2007 *Phys. Rev.* E **75** 061306
[36] Vega Reyes F, Garzó V and Santos A, 2008 *J. Stat. Mech.* P09003
[37] Goldhirsch I and Sela N, 1996 *Phys. Rev.* E **54** 4458
[38] Sela N, Goldhirsch I and Noskowicz S H, 1996 *Phys. Fluids* **8** 2337
[39] Sela N and Goldhirsch I, 1998 *J. Fluid Mech.* **361** 41
[40] Lutsko J F, 2004 *Phys. Rev.* E **70** 061101
[41] Vega Reyes F, Santos A and Garzó V, 2010 *Phys. Rev. Lett.* **104** 028001
[42] Vega Reyes F, Garzó V and Santos A, 2011 *Phys. Rev.* E **83** 021302
[43] Bird G I, 1994 *Molecular Gas Dynamics and the Direct Simulation of Gas Flows* (Oxford: Clarendon)
[44] Dufty J W, Brey J J and Santos A, 1997 *Physica* A **240** 212
[45] Brilliantov N V and Pöschel T, 2004 *Kinetic Theory of Granular Gases* (Oxford: Oxford University Press)
[46] Tij M, Tahiri E E, Montanero J M, Garzó V, Santos A and Dufty J W, 2001 *J. Stat. Phys.* **103** 1035
[47] Burnett D, 1934 *Proc. London Math. Soc.* **40** 382
[48] Lockerby D A and Reese J M, 2003 *J. Comput. Phys.* **188** 333
[49] Garzó V and Santos A, 2003 *Kinetic Theory of Gases in Shear Flows. Nonlinear Transport* (Dordrecht: Kluwer Academic)
[50] Santos A, Garzó V and Vega Reyes F, 2009 *Eur. Phys. J. Spec. Top.* **179** 141
[51] Cercignani C, 1988 *The Boltzmann Equation and Its Applications* (New York: Springer)
[52] Brey J J, Dufty J W and Santos A, 1999 *J. Stat. Phys.* **97** 281
[53] Frezzotti A, 1997 *Phys. Fluids* **9** 1329

doi:10.1088/1742-5468/2011/07/P07005

J. Stat. Mech. (2011) P07005

[54] Montanero J M and Santos A, 1997 *Phys. Fluids* **9** 2057
[55] Montanero J M, Garzó V, Santos A and Brey J J, 1999 *J. Fluid Mech.* **389** 391
[56] Astillero A and Santos A, 2005 *Phys. Rev.* E **72** 031309
[57] Vega Reyes F, Garzó V and Santos A, *Rheological properties of a granular impurity in the Couette flow*, 2008 *The XVth Int. Congr. on Rheology (Melville, NY)*; *AIP Conf. Proc.* **1027** 953

J. Stat. Mech. (2011) P07005